Solution Behavior of Rod-Like Polyelectrolyte-Surfactant Aggregates Polymerized from Wormlike Micelles

Daniel M. Kuntz and Lynn M. Walker*

Department of Chemical Engineering (Center for Complex Fluids Engineering), Carnegie Mellon University, Pittsburgh, Pennsylvania 15213

Received: December 21, 2006; In Final Form: March 7, 2007

The behavior of a rod-like, water-soluble, polyelectrolyte−surfactant aggregate system ($pC_{16}TVB$) in aqueous solution is characterized to determine the partitioning of surfactant in these systems and the impact on aggregate structure. These aggregates are generated by in situ polymerization of a cationic surfactant−hydrotrope wormlike micelle system. This system differs from most other polyelectrolyte-surfactant systems in that the monomer groups and the surfactant are present in ion pairs in the absence of added salts or counterions, so the stoichiometry (with respect to charge) is 1:1 for the system. Therefore, after polymerization the surfactant acts as the counterion for the polyelectrolyte chains as other counterions (salts) are not available. Despite being present in a 1:1 molar ratio, the aggregates are surprisingly stable in water (concentrations >600 mg/mL have been achieved). The conformation of the polyelectrolyte in the aggregate is analogous to the case of a polymer chain in tight confinement in a "tube" or cylindrical pore in which the pore walls are attractive—the tube is formed by the surfactant which is free to dissociate from the aggregates. A simple model for the structure and partitioning is presented and the ability to manipulate the aggregate structure is demonstrated.

Introduction

In oppositely charged polyelectrolyte (PE)−surfactant (S) systems, the balance of hydrophobic and electrostatic interactions between the two species determines the structure and solution behavior of the system. In many systems, the electrostatic attraction dominates surfactant−polyelectrolyte interactions leading to precipitation of insoluble aggregates, often to form materials with interesting nanoscale structure.[1−5] Even in systems that do not show precipitation, the resulting phase behavior is rich, including the formation of gels[6] and immiscible liquid−liquid phases.[7−9] Generally, these effects are seen near the point that the stoichiometry of the complexes, with respect to charge, is 1:1.[1,7] In most previously studied systems, the PE and surfactant are prepared separately and mixed in solution. Therefore, the counterions on the PE and surfactant species are involved in the aggregation of the complexes, both through competition for binding sites and shielding of electrostatic interactions within the complexes and between them.

In the work discussed here, we investigate the structure in aqueous solution of a system in which the PE chain is generated from a polymerizable hydrotrope and the only available counterion to the resulting PE is the original surfactant. The chemistry and initial structural characterization has been presented previously,[10−13] and the salient features are discussed briefly here. In the work described here, a micellar template with polymerizable monomers (hydrotropes) is polymerized directly to a PES system. This provides a different approach to PES formation, avoiding long equilibration times for solutions, and allows for control of the stoichiometry and counterion chemistry. Since the PE chain is grown from charged monomers available in a 1:1 stoichiometry with the surfactant, the result is a system of PES aggregates with no small-ion salts present at any point in the complex formation. The aggregates are soluble and extremely stable in water over a wide concentration range despite being present at a stoichiometry of 1:1. Other examples of polymerization of surfactant-hydrotrope materials exist. An approach similar to ours polymerizes the surfactant molecule itself forming a bottle-brush PE with hydrotrope counterions; this system also results in stable, water-soluble aggregates but represents a PE-counterion and not a PES system.[14,15]

In solution, the unpolymerized "template" forms entangled worm-like micelles. The formation of elongated, threadlike micelles in mixtures of these types of surfactants and counterions is expected and observed in many similar systems.[16−19] The micelles are formed by self-association of a cationic surfactant (cetyltrimethylammonium, $C_{16}TA^+$) and a hydrotropic anionic monomer (4-vinylbenzoic acid, VB^-) that, in this case, happens to be a suitable monomer for polymerization. Due to this self-assembly process, a high local concentration of vinylbenzoic acid (VB^-) monomer exists in the micelle core among the surfactant ($C_{16}TA^+$) alkane tails. The high monomer concentration in the micelle core (∼1.5 M) facilitates polymerization and leads to typical conversion rates near 96%. The length of the resulting aggregates is controlled by the polymerization conditions and can be varied from less than 100 nm to greater than 350 nm by varying initiator concentration, initiator decay time, and reaction temperature.[12] The corresponding diameter of the aggregates is 4 nm and is controlled by the surfactant template, with the aggregate diameter being the same as the original micelle template.[11−13,20] NMR results on the micelle template indicate that the carboxyl group of the VB^- monomer resides at the organic/water interface with the vinyl group extending into the micelle core[12] while kinetic studies of the reaction propagation show rates similar to microemulsion polymerization of styrene.[11] These results indicate that the vinyl groups are initially in the alkane core of the micelle and that the polyelec-

* To whom correspondence should be addressed. E-mail: lwalker@andrew.cmu.edu.

10.1021/jp0688308 CCC: $37.00
Published on Web 05/24/2007

TABLE 1: Comparison of SLS and GPC Data Previously Published[11] [a]

SLS			GPC			comparison	
$M_{w,agg}$	$R_{g,z}$	L_{RR}	$M_{w,pVB}$	$M_{z,pVB}$	$L_{c,z}$	$0.34 \cdot M_{wagg,SLS}/M_{w,GPC}$	$L_{c,GPC}/L_{RR,SLS}$
437 000	36	124	108 000	172 000	413	1.4	3.3
520 000	40	138	100 000	143 000	344	1.8	2.5
730 000	43	150	210 000	358 000	861	1.2	5.7
1 300 000	70	242	368 000	790 000	1900	1.2	7.9

[a] All length and radius of gyration (R_g) measurements are in units of nm and molecular weight (MW) measurements are in units of g/mol. Explanation of columns is as follows: SLS Parameters: $M_{w,agg}$, the weight-averaged MW of $pC_{16}TVB$ aggregates; $R_{g,z}$, the *z*-averaged radius of gyration of $pC_{16}TVB$ aggregates; L_{RR}, the aggregate length calculated from $R_{g,z}$ assuming a rigid rod. GPC parameters: $M_{w,pVB}$, the weight-averaged MW of pVB^-; $M_{z,pVB}$, the *z*-averaged MW of pVB^-; $L_{c,z}$, contour length of pVB^- chain calculated from $M_{z,pVB.}$ comparison $-$ $0.34 \cdot M_w$ agg; SLS/$M_{w,GPC}$, comparison of pVB^- M_w measurements; $L_{c,GPC}/L_{RR}$, comparison of GPC contour length of pVB chain and SLS aggregate length.

trolyte grows in the core of the micelle, probably near the inner organic/ water interface, and not on the outer surface of the micelle.

The resulting high aspect-ratio aggregates are comprised of a pVB^- polyelectrolyte chain (carboxylated polystyrene) for which the $C_{16}TA^+$ molecules now act as counterions. Comparison of static light scattering (SLS) results for the aggregates and gel permeation chromatography (GPC) results for the PE chains alone (in modified form suitable for GPC) has shown that the longer aggregates ($L > 120$ nm) are comprised of approximately one chain per aggregate.[11] Table 1 lists measured parameters from GPC and SLS for a range of samples; these data have been published previously.[11] A simple mass balance is performed by comparing the molecular weight of the pVB^- chain inside an aggregate (which composes 0.34 times the aggregate molecular weight based on the molecular weights of VB^- and $C_{16}TA^+$ given the 1:1 molar ratio) measured directly using a full Zimm analysis (SLS), to the molecular weight of the PE chain with the surfactant removed, measured directly with GPC. The ratio of the appropriate molecular weights is provided in the second column from the right in Table 1 and is essentially equal to 1, indicating that there is one PE chain per aggregate.

In solution, the aggregates exhibit a rigid, cylindrical structure and this structure has been confirmed using scattering methods.[11,13] Comparison of GPC and SLS results reveals that the pVB^- chain within an aggregate is neither fully extended nor completely coiled; rather, it adopts a conformation in between these two limiting cases.[11,20] Comparison of GPC contour length to SLS aggregate length given in Table 1 shows that the chain within an aggregate cannot be fully extended as the contour length of the PE chain is as much as an order of magnitude greater than the aggregate length. It is assumed that the resultant pVB^- chain conformation represents an equilibrium structure arising from interactions with the surfactant counterions and confinement of the chain to the aggregate. NMR results[11] indicate that some fraction of the surfactant counterion remains mobile after polymerization. The fact that surfactant is partitioned between the aggregates and bulk solution suggests that the ratio of surfactant to charged monomer groups on the chains will vary with aggregate concentration and solution properties. Here, we detail the colloidal behavior of these aggregates in aqueous solution and the impact of the variation of stoichiometry on the aggregate structure. We present a structural picture for the aggregates, one in which we envision a hydrophobic PE chain solubilized in a "tube" of surfactant much like a PE in a cylindrical pore with attractive walls. The aggregate represents an equilibrium structure with surfactant free to partition between free solution (and the air−liquid interface) and the aggregate. The water-insoluble PE chain does not partition or dissociate and acts to anchor the aggregate.

Materials and Methods

Surfactant−Monomer Preparation. The surfactant/ counterion pair, cetyltrimethylammonium 4-vinylbenzoate ($C_{16}TVB$), used for this work is synthesized from commercially available cetyltrimethylammonium bromide, or $C_{16}TAB$ (98% purity, BDH Limited, Poole, UK) via two counterion exchange steps. Initially, a 10 wt % solution of $C_{16}TAB$ in methanol is prepared. To replace the bromide counterion (Br^-) of the surfactant with a hydroxide counterion (^-OH), this solution is passed through a column containing an ion-exchange resin (DOWEX monosphere 550 Å anion exchange resin, ^-OH conversion 99%, Sigma-Aldrich). Each $C_{16}TAB$/methanol solution is passed through a column containing excess exchange resin multiple times to ensure high conversions to $C_{16}TAOH$, and conversion is verified by measuring pH (values greater than 12). Methanol solvent is removed under vacuum and the solid $C_{16}TAOH$ crystals are suspended in deionized water at 10 mg/mL for the second ion-exchange step. Here, the ^-OH counterion is replaced with the polymerizable 4-vinylbenzoic monomer via a neutralization reaction. The 4-vinylbenzoic acid (97%, Aldrich) is dissolved in a minimal amount of acetone and added to a 10 mg/ mL $C_{16}TAOH$/water solution while stirring. The solution is chilled in an ice water bath during the exchange process to keep the temperature below the Kraft temperature of $C_{16}TVB$ ($\sim$19 °C) but above the Kraft temperature of $C_{16}TAOH$ ($<$0 °C), and the solution is allowed to exchange with stirring for 3 h. In this manner, as $C_{16}TVB$ is formed, it is precipitated, and a high conversion can be achieved. The mixture is then refrigerated ($T < 19$ °C) to allow the $C_{16}TVB$ crystals to settle out for subsequent separation, washing, and filtration followed by drying under vacuum. Purity of the $C_{16}TVB$ product has been verified by NMR.[11,13]

Polymerization−Formation of PES Complexes. The dried $C_{16}TVB$ is suspended in deionized water at 10 mg/mL ($\sim$1 wt %) in preparation for free radical polymerization. To minimize the presence of free radical scavengers in the reaction, all water solutions are boiled and then bubbled with nitrogen (grade 5.0) and the entire reaction process is performed under nitrogen (grade 5.0). The reaction mixture, a viscoelastic, wormlike micellar solution, is allowed to stir and homogenize at 60 °C. Once the $C_{16}TVB$ has dissolved and the solution has homogenized, the reaction is initiated using the aqueous soluble initiator 2,2′-azobis[2-2(imidazolin-2-yl) propane] dihydrochloride, or VA-44, (Wako Chemicals USA, Inc., Richmond, VA). The amount of added initiator governs the average length of the aggregates because the initiator controls the molecular weight of the PE chains which, in turn, dictate the length of the aggregates.[11,12] The aggregates in this work were synthesized using a fixed amount of initiator (2.5 mol % relative to the amount of surfactant) which generates aggregates ranging from 130 to 150 nm in average length. There is some batch to batch variation in the molecular weight of the PE chains, and the product of each batch is fully characterized for aggregate dimensions and conversion prior to use. The specific batch used in this work has an average length of 140 nm as measured by SLS (experimental results have been confirmed on samples from

additional batches but are not shown). The reaction proceeds with stirring for 3 h to ensure high conversion (typically as high as 96%, verified via titration against bromine[20]), yielding the polymerized product, $pC_{16}TVB$.[11]

Structural Properties of Complexes. For preparation of surfactant-depleted samples, a solution of $pC_{16}TVB$ was placed in dialysis tubing (6−8000 g/mol cutoff Spectra/Por Membrane tubing, Spectrum Laboratories, Inc.), and the tube was placed in a container of fresh deionized water (pH was not controlled, however no large pH changes were detected). The water on the outside of the tube was replaced five times over a span of nearly 3 weeks to promote removal of the surfactant counterion ($C_{16}TA^+$). After dialysis, the material was collected and freeze-dried. The amount of surfactant removed could not be easily quantified, so a large batch was dialyzed and the actual composition determined by titration and comparison to the original 1:1 $pC_{16}TVB$ sample (see discussion of Figure 5). Surfactant-rich samples were prepared by the addition of a small volume of $C_{16}TAB$ solution to the original 1:1 $pC_{16}TVB$ solution.

$pC_{16}TVB$ solutions are characterized using a variety of techniques. Average length and molecular weight, as well as the second virial coefficient, are obtained by static light scattering (SLS). Static light scattering measurements were made with a Brookhaven Instruments Corporation BI-200SM goniometer using a vertically polarized laser ($\lambda = 532$ nm). The samples were placed in borosilicate scintillation vials (Fisher, sample path length ~2.5 cm) for measurements and were referenced against scattering from a toluene standard ($R_{toluene} = 3.50 \cdot 10^{-5}$ 1/cm). The typical scattering angle range used was 70°−130°, and the d*n*/d*c* value for $pC_{16}TVB$ in H_2O ($1.92 \cdot 10^{-7}$ m^3/g) was measured using a differential refractometer. For the surfactant-rich system, a dn/dc value of $1.99 \cdot 10^{-7}$ m^3/g was measured. Solution concentrations were confirmed via UV−vis comparison to known solutions on a Spectronic Genesys 2 UV−vis spectrophotometer ($\lambda = 296$ nm). UV−vis measurements concomitantly provide a method for detecting any low-conversion reactions.

To obtain the hydrodynamic size of the aggregates, dynamic light-scattering (DLS) measurements were preformed on dilute $pC_{16}TVB$ solutions at various conditions. Initially, multi-angle DLS experiments were preformed on two limiting cases to confirm that the observed aggregate diffusion was dominated by translational self-diffusion. Multi-angle DLS measurements were made using the Brookhaven Instruments Corporation instrument mentioned above at a temperature of 25 °C and a concentration of 1 mg/mL. Correlation functions at angles between 30° and 150° were collected. Samples were allowed to correlate for 10 min per measurement and analysis of the correlation functions was preformed using the CONTIN method with an initial delay time of 1.0 μs and a final delay time of 100 μs. In some cases an initial delay time of 2.4 μs was used to eliminate afterpulsing effects in the early time scales of the correlation function. The average relaxation time frequency, $\Gamma(q)$, was obtained for each sample from ten individual runs at each angle. $\Gamma(q)$ was plotted against q^2 to verify the dominance of translation and lack of rotational diffusion. $\Gamma(q)$ for two systems representing extremes in size show a linear dependence in q^2 with a regression passing through the origin (see Supporting Information Available, Figure S1), indicating that diffusion in this range is dominated by translational self-diffusion and any rotational diffusion effects are negligible.[21] Following the relationship, $\Gamma(q) = D_o \cdot n_o^2 \cdot q^2$, where D_o is the apparent diffusion coefficient, n_o is the refractive index of the solvent, and q is as defined in SANS, the apparent diffusion coefficient for each sample is determined from the regression of the data.

Having verified the lack of rotational diffusion effects at these length scales, solution behavior and counterion effects in dilute $pC_{16}TVB$ solutions were explored by measuring aggregate diffusion via DLS measurements at a single angle. Apparent diffusion coefficients for the two samples shown in Figure S1 were found to be slightly lower (~10%) than those measured from the full q^2 dependence. These single-angle measurements were made using a Malvern Zetasizer-Nano Series instrument which uses backscatter geometry with a scattering angle of 173°. The laser wavelength on the instrument was 532 nm, and disposable optical cuvettes with 1 cm path length were used. The correlator on the instrument probed times of 500 nanoseconds and greater. For all DLS measurements presented (multi-angle and single-angle), a single-exponential decay is seen in the auto-correlation function. We do not observe the so-called "slow mode" phenomenon often observed in PE solutions.[22]

Surface tension measurements were performed using a Du Nouy ring at ambient temperature. Surface tension is often used as a measure of the solution behavior of simple surfactant systems.[23] This technique provides a measure of the adsorption of surfactant at the liquid/vapor interface which is an indirect measure of the partitioning of surfactant between the interface and the amount of free surfactant in solution. For simple surfactants, this experiment allows for determination of the critical micelle concentration (CMC). In polymer−surfactant systems, this type of experiment is also used to identify the critical aggregation concentration (CAC) and point of saturation of the polymer.[3,24,25]

Small-angle neutron scattering (SANS) experiments were employed to probe smaller length scales, such as particle cross section or diameter (4 nm) and to obtain information about particle shape at the 10−100 nm scale. SANS measurements were made at the National Institute of Standards and Technology (NIST) Center for Neutron Research in Gaithersburg, MD. All measurements were made on the NG3 30-meter SANS instrument using three sample-to-detector distances (1.5, 4.5, and 13.1 m) providing a q-range of 0.003 to 0.4 1/Å, where $q \equiv 4\pi/\lambda \sin(\theta/2)$. The beam was comprised of neutrons of wavelength 6 Å ($\Delta\lambda/\lambda = 0.150$) and the sample path length was either 1 or 2 mm in quartz sandwich cells. After correction for empty cell scattering and background scattering the data sets were circularly averaged and processed using software supplied by NIST.[26]

Results

Small-angle neutron scattering (SANS) was used to characterize the local nanometer structure of the aggregates in solution. Scattered intensity, $I(q)$, as a function of scattering angle, q, for $pC_{16}TVB$ solutions of different concentrations in D_2O is shown in Figure 1. For solutions of 1 mg/mL in D_2O, the scattering is reminiscent of a cylindrical object with a q^{-1} region ($3 \cdot 10^{-3}$ to $5 \cdot 10^{-2}$ 1/Å) and turn-over at higher q ($q > 5 \cdot 10^{-2}$ 1/Å) due to the finite cylindrical cross-section.[27] Similar SANS results for these aggregates have been observed and successfully modeled as a rigid rod with a cylindrical cross-section.[13,20] For the data shown, a value of the cross sectional radius, 4 nm, is extracted from this region through a Guinier analysis.[11,13] The solid line represents the predicted form factor for rigid, monodisperse, rod-like objects (4 nm in diameter, length greater than ~100 nm). As seen in the figure, the scattering data from a dilute (1 mg/mL) solution of $pC_{16}TVB$ aggregates agrees well with the model over the q-range displayed. SANS from a 0.1

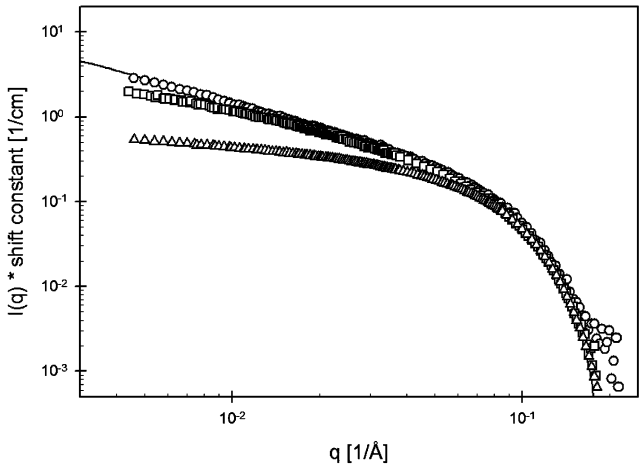

Figure 1. Scattering intensity of neutrons as a function of scattering angle q for a series of concentrations of $pC_{16}TVB$. The intensity has been shifted to demonstrate the common high-q shape ($q > 5 \cdot 10^{-2}$ 1/Å). Data from 1 (○), 10 (□), and 100 mg/mL (△) solutions. The solid line represents model scattering from rigid, monodisperse cylinders of diameter 4 nm and length of 140 nm. The shift constants for the data are 1.15, 0.25, and 0.01 for 1, 10, and 100 mg/mL, respectively.

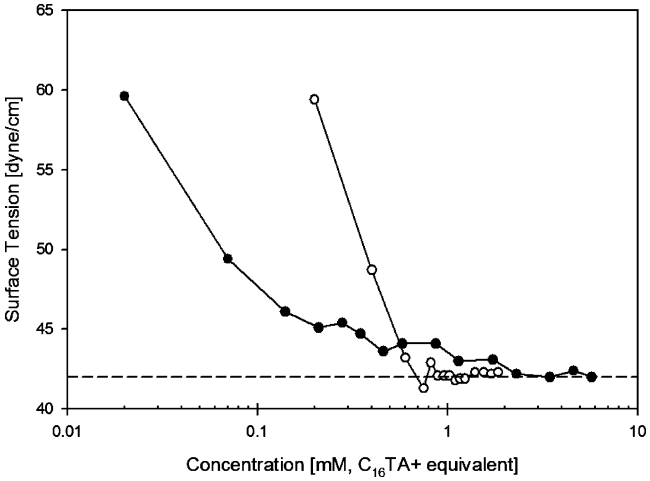

Figure 2. Surface tension of $C_{16}TAOH$ (○) and $pC_{16}TVB$ (●) data, respectively. The data for $pC_{16}TVB$ covers a concentration range of 0.01 mg/mL to 2.5 mg/mL.

mg/mL solution yields a curve of the same shape (not shown). Therefore, concentrations of approximately 1.0 mg/mL (and below) represent the "dilute regime" for the $pC_{16}TVB$ system. While the radial dimensions of the aggregates are determined from SANS, the available q-range is not low enough to accurately model aggregate length from SANS data. The average aggregate length as determined from SLS measurements from dilute solutions was found to be 140 nm assuming a rigid rod conformation ($R_{g,z} = 42$ nm, where $L_{rod} = (12 \cdot R_{g,z}^2)^{1/2}$). We utilize light scattering to characterize aggregate length and SANS to characterize the local rigidity and cross section of the aggregates.

As aggregate concentration is increased, the contribution of interparticle interactions is observed at lower q-values as seen in Figure 1. As aggregate concentration is increased, the deviation from the model at low-q increases as evidenced by the 10 and 100 mg/mL scattering curves. Though the detailed nature of the particle−particle interactions is unclear, second virial coefficient measurements (typical values $\sim 1.0 \cdot 10^{-4}$ cm^3·mol/g^2 from SLS measurements) and depression of SANS intensity at low q indicate repulsive interactions, most likely dominated by steric interactions.[20] Despite the interparticle interactions, at high q-values the data for all concentrations (at this time measured as high as 600 mg/mL, data not shown) collapses and agrees with the simple rigid cylinder model, indicating that the particle cross-section is maintained as concentration is increased.

While $pC_{16}TVB$ aggregates adopt a rod-like structure in solution, they cannot be treated simply as a system of solid rod-like particles. Since the "surfactant counterion" on the PE chain in the system is mobile and an integral part of the aggregate structure, its solution behavior has significant effects on the overall aggregate structure. Surface tension is used to explore the surfactant solution behavior in $pC_{16}TVB$ solutions. The results are shown in Figure 2 as a plot of surface tension versus effective surfactant concentration. The open symbols correspond to solutions of pure surfactant ($C_{16}TAOH$) without polymer. Here, a slope change in the surface tension with increasing concentration is seen as expected. The CMC of the pure surfactant occurs at 0.25 mg/mL $C_{16}TAOH$ (equivalent to 0.8 mM $C_{16}TA^+$, this value is in agreement with literature values for $C_{16}TA^+$ in the presence of small ions[28,29]). In comparison, the closed symbols represent the $pC_{16}TVB$ data. Although no clear CAC is observed in this data, the decline in surface tension and gradual approach to the surface tension of the pure surfactant is evident. The fact that the surface tension is a function of $pC_{16}TVB$ concentration demonstrates that below 2.3 mM $C_{16}TA^+$ equivalent (1 mg/mL $pC_{16}TVB$), the $C_{16}TA^+$ is partitioned between aggregates, free solution, and the interface and that this balance changes as the overall concentration of aggregates varies. At higher concentrations, the aggregates coexist with a fixed concentration of free surfactant in solution (a concentration roughly equivalent to the CMC of $C_{16}TA^+$); as the concentration decreases a region of overall concentration is reached where the surfactant is forced to leave the aggregates to maintain the concentration of surfactant in free solution. This partitioning results in a net negative charge for the aggregates as the cationic surfactant leaves the aggregates to replenish the free solution equilibrium.

Since the surfactant in the system partitions between surfactant free in bulk solution and surfactant bound to the aggregate, the aggregate structure is sensitive to the relative amounts of surfactant and polyelectrolyte present in the system. To probe the system sensitivity to surfactant concentration and the effect of the disturbing the $C_{16}TA^+$:VB^- ratio, surfactant-depleted and surfactant-rich systems were prepared and structurally characterized using light scattering and SANS. Dilute solution (1 mg/mL) SANS data for these systems along with the 1:1 system are shown in Figure 3. The solid lines represent model scattering from rigid, monodisperse, cylinders (4 nm in diameter, varied length). For the 1:1 system, this is the same data as was shown in Figure 1.

As seen in Figure 3, the surfactant-rich system (0.75 mM $C_{16}TAB$ added, 1.3:1 molar ratio of surfactant to monomer units) deviates from the 1:1 curve at low q-values. The low q scattering seen in the surfactant-rich (1.3:1) system is indicative of a decrease in aggregate length. The change at low q is well described by a rigid rod model with a shorter length ($L = 30$ nm) as shown in the figure. The scattering profiles cannot be effectively modeled assuming that spherical micelles of excess surfactant have formed, nor has evidence of spherical micelle formation been detected. Despite the decrease in length, the radial cross section (high-q data) is unchanged as is the negative one (q^{-1}) slope in the intermediate q-range. The rod-like nature of the aggregates is undisturbed, but the average length decreases

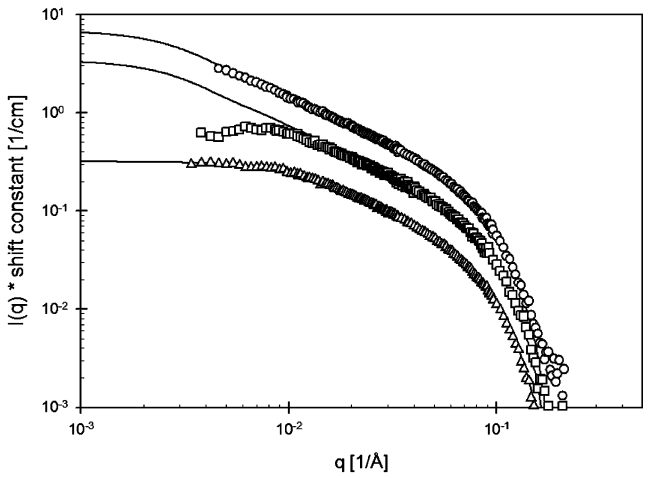

Figure 3. SANS data from dilute $pC_{16}TVB$ solutions (1 mg/mL). Data for 1:1 (○), surfactant-depleted (□), and surfactant-rich (△) solutions. Solid lines represent model scattering from rigid, monodisperse cylinders of diameter 4 nm and varied length. The model curves for the 1:1 and surfactant-depleted data (top two model curves) are of length 140 nm. The model curve for the surfactant-rich data (bottom curve) is of length 30 nm. The 1:1 and surfactant-rich model curves are unshifted and the shift constant (arbitrary) for the depleted model is 0.42. The shift constants for the data are 1.15, 0.19, and 0.35 for the 1:1, surfactant-rich, and surfactant-depleted systems, respectively.

by a factor of nearly five; the aggregates have "compressed", but only in one dimension. Additional surfactant condensed on the surface of the aggregates is likely decreasing any repulsive interactions between monomer groups on the PE allowing the chain to collapse within the aggregate.

The surfactant-depleted system (surfactant removed to result in 0.17 mM or 0.93:1 molar ratio of surfactant to monomer units) also deviates from the scattering of the 1:1 system at low q-values. As seen in Figure 3, a weak correlation peak at about $q = 5 \cdot 10^{-3}$ 1/Å followed by an apparent up-turn is seen in the surfactant-depleted system. However, the rod-like nature and cross-section of the aggregates are undisturbed as the data at intermediate and high q-values is unchanged. As aggregate concentration is increased, this correlation peak lessens and is completely depressed at 100 mg/mL as shown in Figure 4. If depletion of the surfactant from the system leads to an increased number of unbalanced PE groups, we would expect a more charged aggregate and the peak in the 1 mg/mL scattering could be attributed to interparticle Coulombic replusion. However, this peak would be expected to shift as concentration is increased, rather than simply decrease and flatten, so a change in the charge of the rods alone cannot account for the behavior.

The addition of surfactant to the 1:1 system changed the length of the aggregates, but we cannot use SANS to characterize longer aggregates—so another approach is required to determine if the dimensions of the aggregates increase when surfactant is removed. We employ dynamic light scattering (DLS) to measure aggregate diffusion and estimate overall size. We assume that diffusion data reflects mainly changes in aggregate length as SANS data at all system conditions presented showed that the cross-section, or radial dimension, of the aggregates remains constant as does the apparent rod-like nature (I vs q slope of -1). In addition, SANS data (Figure 3) shows evidence of a decrease in aggregate length in the 1.3:1 system. Without a direct structural measure, we can only assume that changes in translational diffusion (measured by DLS) are due to changes in aggregate length; however, we will simply report apparent diffusion coefficient (D_o) to compare different systems.

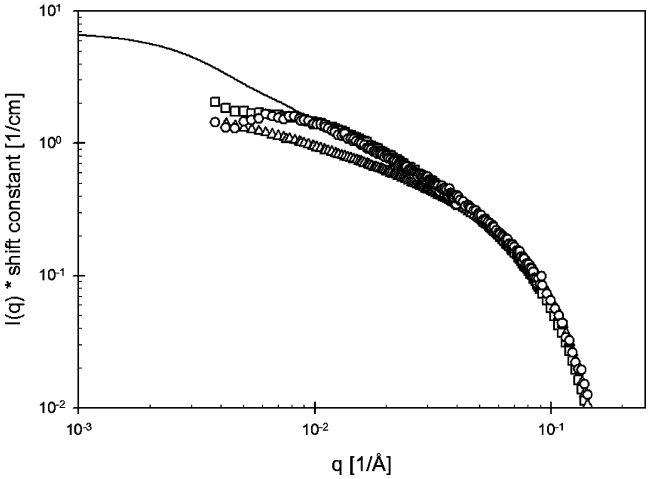

Figure 4. Scattering intensity of neutrons for a series of concentrations of surfactant-depleted $pC_{16}TVB$. The intensity has been arbitrarily shifted to demonstrate the high-q overlap. Data from 1 (○), 10 (□), and 100 mg/mL (△) solutions. The solid line represents model scattering from rigid, monodisperse cylinders of diameter 4 nm and length 140 nm. The shift constants for the data are 0.90, 0.17, and 0.021 for 1, 10, and 100 mg/mL, respectively.

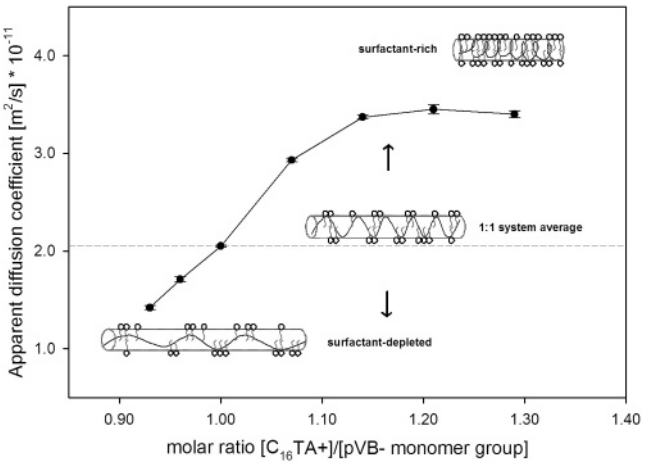

Figure 5. DLS data from a 1 mg/mL $pC_{16}TVB$ solution with varied amounts of surfactant present. The molar ratio of components has been estimated by comparison to 1:1 DLS data. The left-most data point is from a surfactant-depleted system and subsequent points have increasing amounts of added surfactant present.

The observed dependence of aggregate size on $C_{16}TA^+$:VB^- ratio allows us to "titrate" the structure of the aggregates by varying the amount of surfactant present in the system. An example of this experiment can be seen in Figure 5. Here, after surfactant depletion by dialysis, increasing amounts of $C_{16}TA^+$ (in the form of $C_{16}TAB$) were added to the solution while the aggregate concentration was held constant at 1.0 mg/mL. The data is plotted as a function of molar ratio of $[C_{16}TA^+]/[VB^-]$ present in the system. Values of D_o measured for undialyzed 1:1 samples were used to place the titration curve on the correct molar ratio axis. As the amount of $C_{16}TA^+$ present in the system is increased, a marked increase in D_o is seen. At $[C_{16}TA^+]/[VB^-]$ ratios above about 1.15 the D_o curve levels off. Here, the system has reached a saturated state in terms of aggregate size. This behavior suggests the presence of critical collapse or coiling of the pVB^- chain at which point the resultant aggregate length ceases to decrease. From SANS, we know that this minimum length is 30 nm. The behavior is reversible and provides a material with a nanoscale dimension that is sensitive to local amphiphile concentration.

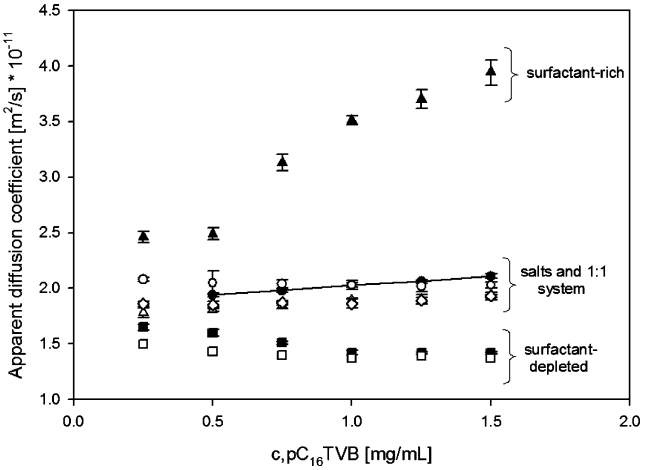

Figure 6. DLS data for $pC_{16}TVB$ solutions of varied concentration with added counterions. Data for systems with added salts are represented by open symbols and data for systems of varied surfactant are represented by closed symbols. Specifically, surfactant-depleted (■), 1:1 (●), and surfactant-rich (▲) data. Open symbols for the same systems with added salts: depleted + 1.25 mM NaBr (□), 1:1 + 0.75 mM NaBr (△), 1:1 + 0.75 mM $MgCl_2$ (◇), and 1:1 + 25 mM NaBr (○). Each data point represents the average over multiple measurements.

To better characterize the impact of solution properties on the aggregate structure, DLS measurements were made on a range of dilute $pC_{16}TVB$ aggregate solutions of various concentrations for the three different surfactant ratios studied. The comparison is shown in Figure 6. First, it is clear that the aggregate size is constant in this range of concentration for the 1:1 system. Since SANS showed that the radius and local rigidity are also constant, we note that the structure of the aggregates is not significantly changed by concentration (even though the partitioning of the surfactant is changing in this concentration range). In the surfactant-depleted DLS measurements the value of D_o decreases slightly and flattens as aggregate concentration is increased. For the surfactant-rich system, D_o increases significantly with $pC_{16}TVB$ aggregate concentration at concentrations above 0.5 mg/mL. Though the data is not shown, the same effect was confirmed upon addition of $C_{16}TAOH$ in place of $C_{16}TAB$. This trend is consistent with a decrease in aggregate size similar to that seen in SANS measurements (Figure 3).

Unlike surfactant, the addition of hard ions has no effect on the aggregate structure. In the middle portion of the figure the data from the 1:1 system (bold line) and the 1:1 system with added salts is shown. The results for these systems are very similar and it appears that the effect of adding small amounts of salt (~1 mM) and excess salt (~25 mM) are negligible in terms of aggregate size. Since polyelectrolyte chains have been shown to bind divalent counterions preferentially over monovalent counterions,[30,31] one may expect multivalent salt to have an effect on the structure of $pC_{16}TVB$ aggregates. However, multivalent salt ($MgCl_2$) also has little effect on the aggregate size measured. As the 1.0 mg/mL SANS data from the depleted system shows evidence of inter-aggregate repulsion, it is possible that the observed decrease in D_o is an artifact of repulsive interactions. If these interactions are completely electrostatic, one would expect the addition of salt to lessen or completely suppress the effect. However, no change in D_o is observed upon addition of NaBr. Clearly, salts do not interact with the aggregates or alter any interparticle interactions in the same manner as the surfactant.

Discussion

On the basis of the results presented, we propose a simple structural model for $pC_{16}TVB$ aggregates. The system is comprised of a PE chain which is trapped in a "tube" of surfactant. The nature of the surfactant tube and its interaction with the PE chain controls many aspects of the aggregates. The alkane tail length of the surfactant controls the radial dimension of the tube and, therefore, the cross sectional diameter of the aggregates. Previous work in our group demonstrates the effect of changing surfactant tail length.[12] Aggregates synthesized using surfactant with shorter ($pC_{14}TVB$) and longer ($pC_{18}TVB$) alkane tails show a respective decrease and increase in aggregate radial dimension consistent with the removal or addition of two carbon−carbon bonds to the surfactant tail in $pC_{16}TVB$. The surfactant tube also solubilizes the PE chain, which is largely insoluble in water at neutral pH. (The solubilization of the monomer in water increases by a factor of over 10^3 in the presence of the surfactant from <0.25 mg/mL as the sodium salt to > 600 mg/mL as either $C_{16}TVB$ or $pC_{16}TVB$). We observe through exhaustive stepwise dialysis that a sufficient amount of surfactant can be removed to render the pVB^- chains insoluble. Upon addition of $C_{16}TA^+$ (in the form of $C_{16}TAB$ or $C_{16}TAOH$) that replenishes the tube, the pVB^- chains resolubilize. Subsequent characterization (SANS and SLS) of the resolubilized sample agrees with that of the original sample prior to surfactant depletion, suggesting that the polymerized aggregate is an equilibrium structure. This reinforces the picture that one PE chain inhabits each aggregate—the reversibility of the system is inconsistent with multiple chains being kinetically trapped in aggregates.

While the surfactant tube houses the PE chain, the tube itself is dynamic and its behavior is determined by the partitioning of surfactant throughout the system. The mobility of the surfactant is seen in surface tension measurements (Figure 2) and also in NMR results.[11] In this system, a given surfactant molecule must partition among two possible phases: interaction with the PE chain (surfactant tube phase) and dissociation into the free phase (it is assumed that this phase includes the air/water interface). If one considers such a system with an overall 1:1 balance, each monomer unit contains one binding site and there exists one site for each surfactant molecule in the system. When the concentration of aggregates is very low (below the equivalent CMC of the surfactant), neither the aggregates nor the bulk solution is saturated with surfactant. As a result, the aggregates are charged since some fraction of the PE monomer groups will not have corresponding surfactant groups on the aggregate. As aggregate concentration increases, more surfactant is added to the system and partitions between the two phases. Above an aggregate concentration of 1.0 mg/mL (2.3 mM $C_{16}TA^+$), the free phase surfactant concentration remains constant (observed surface tension of aggregate solutions is constant and equal to the value observed above the CMC of the pure surfactant) and the remainder of the surfactant in the system is available for tube formation. In effect, the bulk aqueous solution phase is "filled" and the dissociation driving force has vanished. Therefore, as the concentration of aggregates is increased, the added surfactant partitions to the aggregates. Without competition for surfactant, the solubilization tube can form more efficiently and the aggregates slowly approach charge neutrality.

This simple model may explain the observed interaction peak seen in SANS data for the surfactant-depleted system (see Figure 3). In the presence of a fresh water sink provided during dialysis, the free phase driving force increases due to the increased solvent phase volume. Some amount of surfactant from the tube

phase (from aggregates on inside of dialysis membrane) must dissociate into the bulk in attempt to saturate the clean water phase. Consequently, the aggregates are surfactant-depleted and have an increased surface charge. Consistent with the above model, as the aggregate concentration is increased the tube phase is populated and the aggregates approach charge neutrality. Therefore, upon concentrating a surfactant-depleted system, the aggregate surface charge should diminish and any charge-interaction peaks observed in SANS should disappear. This is in fact what is observed in surfactant-depleted $pC_{16}TVB$ (Figure 4) as aggregate concentration is increased. In effect, the surfactant partitioning compensates for the depletion as the aggregate concentration is increased and the system behaves in a manner similar to the 1:1 system.

The overall structure of the aggregates is one of a rigid rod with the diameter set by the surfactant tail length. The surfactant will create a cylindrical "tube" or "pore" with a positively charged interface (heads) and a nonpolar core (tails). The electrostatic interactions between the charge groups of the PE chain and the oppositely charged head-groups of the surfactant molecules draw the PE to the surfactant tube/water interface. As a result of these interactions, the chain is forced to adopt a conformation that is neither fully coiled nor fully extended. The amount of surfactant present in the tube dictates the strength of the electrostatic attraction and hence the degree to which the PE chain is coiled at the interface. As the tube interface attraction increases (surfactant-rich), the PE charge groups are drawn to it and aggregate length decreases. Likewise, as the attractiveness is decreased (surfactant-depleted) the aggregate length increases. As a result, the observed aggregate length dynamically responds to the surfactant partitioning and can be controlled by varying the $C_{16}TA^+$:pVB^- ratio.

The behavior of the pVB^- chain in the surfactant tube is similar to a confined polymer in the limit of tight confinement. In so-called "tight confinement" systems, the radial dimension of the confinement pore is small when compared to the length of the chain, and the chain is in effect elongated by the confinement.[32−38] The system becomes more complex if the walls of the tube are made to be attractive. In this case, disturbance of the chain distribution in both the axial and radial dimensions is possible depending on the strength of the pore wall attraction. As the attractiveness of the wall is increased, the chain samples more locations near the wall instead of elongating in the center of the confining pore. The observed effect is that the chain coils up around the interface of the wall and its overall length compresses as a result.[37] This phenomenon is consistent with the behavior seen in $pC_{16}TVB$ and may explain the partially elongated conformation of the pVB^- chain in an aggregate. Here the surfactant head-groups make up the attractive wall interface that confines the pVB^- chains and the level of attractiveness is set by the amount of surfactant in the tube phase. While the "wall" in $pC_{16}TVB$ is a soft tube comprised of surfactant and not a rigid cylinder, it has been shown that behavior in soft nanotubes can be similar.[35,36]

In terms of quantifying the proposed solution behavior model, a direct measure of aggregate surface charge, through ζ potential measurements, for example, would be helpful. However, measurements on rod-like systems and interpretation of such data is non-trivial and preliminary measurements have been inconsistent and inconclusive. It may be possible to probe the surfactant counterion solution behavior directly using a surfactant-specific electrode.[39] These experiments may be complicated by the nature of the aggregates themselves, but do offer a method for direct characterization.

Conclusions

$pC_{16}TVB$ represents a previously unstudied region of PE−surfactant interaction. In addition to the added complexity of chain−counterion interactions, the system possesses distinct characteristics arising from the solution behavior of the surfactant that are not seen in salt-counterion systems. In light of other PE−surfactant systems, $pC_{16}TVB$ is surprisingly soluble and stable in water. It is believed that the unique behavior of the counterion in the system is the reason for this stability. A simple structural model for the solution behavior of the surfactant counterion is proposed and discussed.

In addition, the dual binding and solubilization nature of the surfactant counterion on the PE chain has profound effects on chain conformation and overall aggregate structure. The net result is a "compressing" or "coiling" effect of the chain around the inner interface of the surfactant tube not unlike that seen in tightly confined polymer systems in which the pore walls are attractive. Despite the proposed "coiling" structure model, it should be noted that the overall rod-like nature of the aggregates is preserved over all concentrations studied thus far (concentrations up to 600 mg/mL). Tuning these features of PE−surfactant systems offers potential in devising soft materials with solution sensitive properties.

Acknowledgment. This work was supported by the National Science Foundation Grant CTS-0092967. Static light scattering equipment was provided by a grant from the PPG foundation. We would like to acknowledge Malvern Instruments, Inc., for their support with the dynamic light scattering and zeta potential instrumentation in the PPG Industries Colloids, Polymers, and Surfaces (CPS) Laboratory at Carnegie Mellon University. This work utilized facilities supported in part by the National Science Foundation under Agreement No. DMR-0454672. We acknowledge the support of the National Institute of Standards and Technology, U.S. Department of Commerce, in providing the neutron research facilities used in this work.

Supporting Information Available: Multi-angle DLS data displaying the relationship of the average relaxation frequency, $\Gamma(q)$, with q^2 for the 1:1 and surfactant-rich system. The fit to the data is linear and passes through the origin, verifying that the observed apparent diffusion coefficient is dominated by translational diffusion and that rotational diffusion effects are negligible. This material is available free of charge via the Internet at http://pubs.acs.org.

References and Notes

(1) Antonietti, M.; Conrad, J.; Thunemann, A. *Macromolecules* **1994**, *27*, 6007.
(2) Faul, C. F. J.; Antonietti, M. *Adv. Mater.* **2003**, *15*, 673.
(3) Goddard, E. D.; Ananthapadmanabhan, K. P. *Interactions of Surfactants with Polymers and Proteins*; CRC Press: Boca Raton, FL, 1993.
(4) La Mesa, C. *J. Colloid Interface Sci.* **2005**, *286*, 148.
(5) Antonietti, M.; Conrad, J. *Angew. Chem., Int. Ed. Engl.* **1994**, *33*, 1869.
(6) Wang, C.; Tam, K. C.; Jenkins, R. D.; Tan, C. B. *J. Phys. Chem. B* **2003**, *107*, 4667.
(7) Wang, Y. L.; Kimura, K.; Huang, Q. R.; Dubin, P. L.; Jaeger, W. *Macromolecules* **1999**, *32*, 7128.
(8) Morishima, Y.; Mizusaki, M.; Yoshida, K.; Dubin, P. L. *Colloids Surf., A* **1999**, *147*, 149.
(9) Bai, G. Y.; Nichifor, M.; Lopes, A.; Bastos, M. *J. Phys. Chem. B* **2005**, *109*, 518.
(10) Biggs, S.; Kline, S. R.; Walker, L. M. *Langmuir* **2004**, *20*, 1085.
(11) Gerber, M. J.; Kline, S. R.; Walker, L. M. *Langmuir* **2004**, *20*, 8510.
(12) Gerber, M. J.; Walker, L. M. *Langmuir* **2006**, *22*, 941.
(13) Kline, S. R. *Langmuir* **1999**, *15*, 2726.

(14) Liu, S. Y.; Gonzalez, Y. I.; Danino, D.; Kaler, E. W. *Macromolecules* **2005**, *38*, 2482.
(15) Zhu, Z. Y.; Gonzalez, Y. I.; Xu, H. X.; Kaler, E. W.; Liu, S. Y. *Langmuir* **2006**, *22*, 949.
(16) Candau, S. J.; Oda, R. *Colloids Surf., A* **2001**, *183*, 5.
(17) Carver, M.; Smith, T. L.; Gee, J. C.; Delichere, A.; Caponetti, E.; Magid, L. J. *Langmuir* **1996**, *12*, 691.
(18) Hassan, P. A.; Yakhmi, J. V. *Langmuir* **2000**, *16*, 7187.
(19) Magid, L. J. *J. Phys. Chem. B* **1998**, *102*, 4064.
(20) Gerber, M. J. The Characterization of Polymerized Worm-like Surfactant Micelles. Ph.D. Thesis, Carnegie Mellon University, Pittsburgh, PA, 2006.
(21) Phalakornkul, J. K.; Gast, A. P.; Pecora, R. *Macromolecules* **1999**, *32*, 3122.
(22) Sedlak, M.; Amis, E. J. *J. Chem. Phys.* **1992**, *96*, 817.
(23) Hiemenz, P. C.; Rajagopalan, R. *Principles of Colloid and Surface Chemistry*, 3rd ed., revised and expanded; Marcel Dekker, Inc.: New York, 1997.
(24) Jones, M. N. *J. Colloid Interface Sci.* **1967**, *23*, 36.
(25) Goddard, E. D. *J. Colloid Interface Sci.* **2002**, *256*, 228.
(26) *SANS Data Reduction and Imaging Software*; NIST: Gaithursburg, MD, 1998.
(27) Higgins, J. S.; Benoit, H. C. *Polymers and Neutron Scattering*; Oxford University Press: New York, 1994.
(28) Okuda, H.; Imae, T.; Ikeda, S. *Colloids Surf.* **1987**, *27*, 187.
(29) Ralston, A. W.; Eggenberger, D. N.; Harwood, H. J.; Dubrow, P. L. *J. Am. Chem. Soc.* **1947**, *69*, 2095.
(30) Hinderberger, D.; Jeschke, G.; Spiess, H. W. *Macromolecules* **2002**, *35*, 9698.
(31) Manning, G. S. *Q. Rev. Biophys.* **1978**, *11*, 179.
(32) Odijk, T. *Macromolecules* **1983**, *16*, 1340.
(33) Daoud, M.; Degennes, P. G. *J. Phys.* **1977**, *38*, 85.
(34) Gilbert, E. P.; Auvray, L.; Lal, J. *Macromolecules* **2001**, *34*, 4942.
(35) Brochard-Wyart, F.; Tanaka, T.; Borghi, N.; de Gennes, P. G. *Langmuir* **2005**, *21*, 4144.
(36) Avramova, K.; Milchev, A. *J. Chem. Phys.* **2006**, *124*.
(37) Milchev, A.; Paul, W.; Binder, K. *Macromol. Theory Simul.* **1994**, *3*, 305.
(38) Sotta, P.; Lesne, A.; Victor, J. M. *J. Chem. Phys.* **2000**, *112*, 1565.
(39) Xu, R.; Bloor, D. M. *Langmuir* **2000**, *16*, 9555.